

Error Introduced by Common Reorientation Algorithms in the Assessment of Rodent Trabecular Morphometry Using Micro-Computed Tomography

Michael D. Newton ¹, Samantha Hartner,¹ Karissa Gawronski,^{1,2} Tristan Maerz²

¹Orthopaedic Research Laboratories, Beaumont Health, 3601 W. 13 Mile Road, Royal Oak 48073, Michigan, ²Department of Orthopaedic Surgery, University of Michigan, Ann Arbor, Michigan

Received 10 November 2017; accepted 17 April 2018

Published online 10 May 2018 in Wiley Online Library (wileyonlinelibrary.com). DOI 10.1002/jor.24039

ABSTRACT: Quantitative analyses of bone using micro-computed tomography (μ CT) are routinely employed in preclinical research, and virtual image reorientation to a consistent reference frame is a common processing step. The purpose of this study was to quantify error introduced by common reorientation algorithms in μ CT-based characterization of bone. Mouse and rat tibial metaphyses underwent μ CT scanning at a range of resolutions (6–30 μ m). A trabecular volume-of-interest (VOI) was manually selected. Image stacks were analyzed without rotation, following 45° In-Plane axial rotation, and following 45° Triplanar rotation. Interpolation was performed using Nearest-Neighbor, Linear, and Cubic interpolations. Densitometric (bone volume fraction, tissue mineral density, bone mineral density) and morphometric variables (trabecular thickness, trabecular spacing, trabecular number, structural model index) were computed for each combination of voxel size, rotation, and interpolation. Significant reorientation error was measured in all parameters, and was exacerbated at higher voxel sizes, with relatively low error at 6 and 12 μ m (max. reorientation error in BV/TV was 2.9% at 6 μ m, 7.7% at 12 μ m and 36.5% at 30 μ m). Considering densitometric parameters, Linear and Cubic interpolations introduced significant error while Nearest-Neighbor interpolation caused minimal error, and In-Plane rotation caused greater error than Triplanar. Morphometric error was strongly and intricately dependent on the combination of rotation and interpolation employed. Reorientation error can be eliminated by avoiding reorientation altogether or by “de-rotating” VOIs from reoriented images back to the original reference frame prior to analysis. When these are infeasible, reorientation error can be minimized through sufficiently high resolution scanning, careful selection of interpolation type, and consistent processing of all images. © 2018 Orthopaedic Research Society. Published by Wiley Periodicals, Inc. *J Orthop Res* 36:2762–2770, 2018.

Keywords: trabecular morphometry; reorientation; realignment; rotation; interpolation; error

The quantitative determination of trabecular morphometry using micro computed tomography (μ CT) is well-established. In 2010, Bouxsein et al.¹ published consensus guidelines for the use of μ CT to assess bone microstructure, facilitating consistent methodology and reporting of results in studies assessing trabecular or cortical bone morphometry. As part of these guidelines, consistent sample preparation and sample positioning are deemed critical components of a high-quality imaging experiment. While every attempt should be made to physically position all samples in a consistent manner, the degree of accuracy with which this can be achieved may vary from study to study. As such, virtual reorientation/realignment algorithms are commonly employed to position and orient datasets in a consistent virtual reference frame. This reference frame may be the common anatomical planes (i.e., sagittal, coronal, axial) or another, study-dependent reference. In addition to facilitating consistent manual contouring, virtual reorientation is also a critical step for orientation-dependent analyses such as 2D cortical bone assessment, the results of which (e.g., moments

of inertia) are directly related to the orientation of the long bone.

Reorientation algorithms rely on data interpolation to reposition an image from one discrete voxel grid onto another, with the goal of preserving both shape and intensity information. The extent of this preservation is dependent upon voxel size (i.e., image resolution), image quality metrics such as signal-to-noise ratio (SNR), and the type of interpolation method utilized. While interpolation method may vary between different software packages, three interpolation methods commonly utilized are nearest-neighbor (NN), linear, and cubic interpolation (Fig. 1). The extent to which these interpolation methods introduce error in the μ CT-based measurement of bone morphometry is, to date, unknown. To this end, the purpose of this study was to quantify the error introduced by three common interpolation methods in the μ CT-based assessment of trabecular bone morphometry of mice and rats, two commonly employed models for bone characterization, and to quantify how this error varies as a function of imaging resolution, the magnitude of rotation, and the number of planes in which rotation/reorientation occurs.

METHODS

Specimen Procurement and Micro Computed Tomography

As part of two unrelated, institutional animal care and use committee (IACUC)-approved protocols, the femora of ten C57BL/6 mice (aged 16 weeks) and 10 Lewis rats (aged 16 weeks) were dissected to completely remove soft tissue. To facilitate rigid specimen immobilization, transverse cuts

Abbreviations: μ CT, micro computed tomography; BMD, apparent bone mineral density; BV/TV, bone volume fraction; HU, Hounsfield units; NN, nearest neighbor; SMI, structure model index; TbTh, trabecular thickness; Tb.Sp, trabecular spacing; Tb.N, trabecular number; TMD, bone tissue mineral density; VOI, volume of-interest

Conflicts of interest: None.

Correspondence to: Tristan Maerz (T: (734) 936 – 2566; F: (734) 232 – 9622; E-mail: tmaerz@med.umich.edu)

© 2018 Orthopaedic Research Society. Published by Wiley Periodicals, Inc.

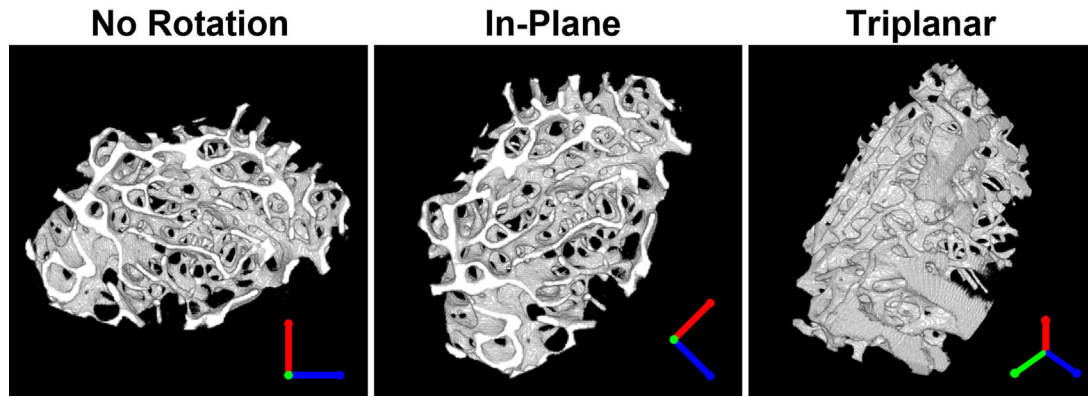


Figure 1. Trabecular volumes derived from image stacks without rotation (Left), following a 45° axial in-plane rotation (Middle), and following a 45° rotation in all three planes (Right).

were made at the level of the third trochanter using a tissue dissection saw. Femora were rigidly mounted in a cylindrical imaging specimen holder such that the long axis of the bone is aligned with the long axis of the specimen holder. During imaging, all samples were completely immersed in room temperature phosphate-buffered saline (pH = 7.4). Imaging was performed at 55 kVp, 145 μ A, 300 ms integration time using a μ CT system (μ CT-40, Scanco Medical, Brüttisellen, Switzerland). The imaging region encompassed 1.25 mm and 2 mm of the distal femoral metaphysis in mice and rats, respectively. This region was consistently selected just below the distal femoral physis and primary spongiosa. Each sample was sequentially imaged at 6 μ m, 12 μ m, 18 μ m, 24 μ m, and 30 μ m voxel sizes. Datasets were exported to DICOM format, imported into MATLAB (r2015a, The Mathworks, Natick, MA), and filtered using a Gaussian filter. Filter kernels were scaled linearly according to voxel size to ensure consistent filtering and to avoid filter-related artifacts within the data. As such, 6 μ m scans were filtered with $\sigma = 0.4$, 12 μ m scans were filtered with $\sigma = 0.2$, 18 μ m scans were filtered with $\sigma = 0.13$, 24 μ m scans were filtered with $\sigma = 0.1$, and 30 μ m scans were filtered with $\sigma = 0.08$.

Image Contouring, Reorientation Algorithms, and Trabecular Morphometry

To segment metaphyseal trabecular bone, manual contouring was performed by an experienced investigator (TM) using a three-plane viewing interface in MATLAB. Sequential contours were morphed using shape averaging to yield one volume of interest (VOI) encompassing only metaphyseal trabecular bone, and VOIs of each image set were saved. To simulate virtual reorientation, a combination of rotations was performed on each sample using MATLAB: No rotation (raw data control), 45° in the axial plane (In-Plane), and 45° in all three planes (Triplanar) (Fig. 1). Rotations were performed using three interpolation types: Linear, Cubic, and NN interpolation (Table 1). This combination of rotations was chosen based on extensive preliminary investigation demonstrating that the extent of interpolation error does not depend on the magnitude of rotation (rotation angle) but rather on whether any rotation is performed. Therefore, to reduce the dataset and simulate the theoretical worst-case rotation, we chose a single rotation magnitude of 45°. In preliminary work, we observed differences between In-Plane and Triplanar rotations and chose to include both types in final analyses. Furthermore, it is common for image sets to

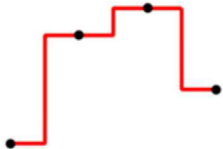


require reorientation/rotation only in a single plane, most commonly the axial plane, which is another rationale for investigating both In-Plane and Triplanar reorientations. The trabecular VOI of each sample was reoriented together with the sample itself, using the identical rotation transform as the sample itself, facilitating consistent analysis within the same VOI to isolate the true effect of image reorientation without confounding effects due to varying VOI size or position.

Bone was segmented from VOIs using resolution- and species-specific thresholds determined by an experienced investigator (TM) using the histogram method as a starting reference and qualitative adjustment thereafter. The final threshold values (6 μ m: 2,800 HU, 12 μ m: 2,750 HU, 18 μ m: 2,725 HU, 24 μ m: 2,700 HU, 30 μ m: 2,675 HU) were optimized to yield consistent relative bone volume fraction (BV/TV) values within each sample across the five different voxel sizes, using the 6 μ m scan as the reference scan. This was done to minimize confounding threshold-dependent effects in our final data set. Trabecular morphometry was performed using boneJ, an open-source plug-in for ImageJ with several standard bone morphometry functions,² and datasets were seamlessly transferred between MATLAB and ImageJ using Miji,³ a MATLAB-ImageJ java interface. Parameters calculated included densitometric and volumetric parameters (hereafter referred to collectively as densitometric) including BV/TV, apparent bone mineral density (BMD), and bone tissue mineral density (TMD), and morphometric parameters including trabecular thickness (Tb.Th), trabecular spacing (Tb.Sp), trabecular number (Tb.N), and structure model index (SMI) were calculated. SMI was computed in boneJ via the Hildebrand and Rüegsegger method, using a mesh smoothing factor of 0.5 and a voxel resampling factor of one and three for mice and rats, respectively.

Statistical Analyses

All statistical analyses were performed in SPSS (v22, IBM, Armonk, NY). First, the equal variance and normality assumptions were confirmed using Levene's test and the Shapiro-Wilk test, respectively. The dataset was surveyed for statistical outliers, of which none were identified. The sphericity assumption was assessed using Mauchly's test of sphericity. The change in morphometric parameters as a function of rotation type (No Rotation, 45° In-Plane, and 45° Triplanar) and interpolation type (Linear, Cubic, Nearest Neighbor) at each voxel size (6, 12, 18, 24, and 30 μ m) was

Table 1. Description of the Three Commonly Employed Interpolation Types for Digital Image Processing Characterized in This Study

Interpolation	1D Illustration	3D Sampling Neighborhood	Description of 3D Implementation
Nearest-Neighbor		$2 \times 2 \times 2$	The value of the closest neighboring voxel is assigned. NN interpolation can only produce exact values present in neighboring voxels.
Linear		$2 \times 2 \times 2$	Trilinear Interpolation. A weighted average of the voxel neighborhood is computed, with linear weighting functions in each dimension. Linear interpolation can only produce values within the range of neighboring voxel values.
Cubic		$4 \times 4 \times 4$	Tricubic convolution. Interpolation is performed using a convolution kernel implementation of cubic curve fitting. Cubic curve fitting can potentially produce values outside the range of neighboring voxel values.

1D illustrations demonstrate determination of interpolated values (red line) lying between known data points (black dots) using each interpolation type.

assessed using three-way repeated measures (RM) analysis of variance (ANOVA). To isolate the true, intrinsic effect of rotation type and interpolation type while controlling for the effect of voxel size, all three factors (rotation type, interpolation type, and voxel size) were defined as within-subject factors in the ANOVA design. Multiple comparisons were then performed using the Bonferroni post hoc test. *p*-values less than 0.001 were considered significant. Percent error was calculated with reference to the non-rotated scan taken at each voxel size—for example, error in an 18 μm , Linear interpolation, Triplanar rotation scan is normalized to the corresponding non-rotated 18 μm scan. This normalization removes the independent effect of voxel size on percent error computation, resulting in error calculations based solely on the effect of the reorientation algorithm.

RESULTS

Generally, observed trends were similar in the mouse and rat datasets. As such, only mouse data is presented. Full graphical absolute results and tabulated percent differences for rat metaphyses are available in the Supplemental Information. $p < 0.001$ can be assumed for all reported significant comparisons. Voxel size had a significant independent effect on BMD, TMD, Tb.Th, Tb.Sp, Tb.N, and SMI. Rotation of any type had a significant independent effect on BV/TV, BMD, Tb.Th, and Tb.N. Interpolation type had a significant independent effect on all densitometric and morphometric parameters. There was a significant three-way interaction between voxel size, rotation, and interpolation type for all densitometric and morphometric parameters, indicating a complex interrelationship between these variables.

Effect of Reorientation Type on Densitometry

Densitometric parameters were not affected by either In-Plane or Triplane rotation when NN

interpolation (Fig. 2C, F, and I) was used. Conversely, when Linear (Fig. 2A, D, and G) or Cubic interpolation (Fig. 2B, E, and H) were used, both In-Plane and Triplanar rotations markedly increased measured BV/TV, BMD, and TMD, with In-Plane rotation generally producing higher error than Triplanar rotation. In the majority of cases, the magnitude of error for a given measurement, rotation type, and interpolation type increased with increasing voxel size (Table 2). BV/TV following In-Plane rotation was significantly higher at all voxel sizes using both Linear (Fig. 2A) and Cubic (Fig. 2B) interpolations, and significantly higher following Triplanar rotation at 6 and 12 μm using Linear interpolation, and at all voxel sizes using Cubic interpolation. In-Plane rotation also resulted in significantly higher BV/TV compared to Triplanar rotation at all voxel sizes using both Linear and Cubic interpolations. BV/TV had the greatest magnitude percent error compared to other densitometric parameters (Table 2). BMD following In-Plane and Triplanar rotations was significantly higher at all voxel sizes using both Linear (Fig. 2D) and Cubic (Fig. 2E) interpolation, and In-Plane rotation resulted in significantly higher BMD compared to Triplanar rotation at all voxel sizes using both Linear and Cubic interpolations. TMD following In-Plane and Triplanar rotations was significantly higher at 6, 12, and 18 μm using Linear interpolation (Fig. 2G) and significantly higher at all voxel sizes using Cubic interpolation (Fig. 2H). In-Plane rotation resulted in significantly higher TMD compared to Triplanar rotation at 6, 12, 18, and 24 μm using Linear interpolation and at all voxel sizes using Cubic interpolation.

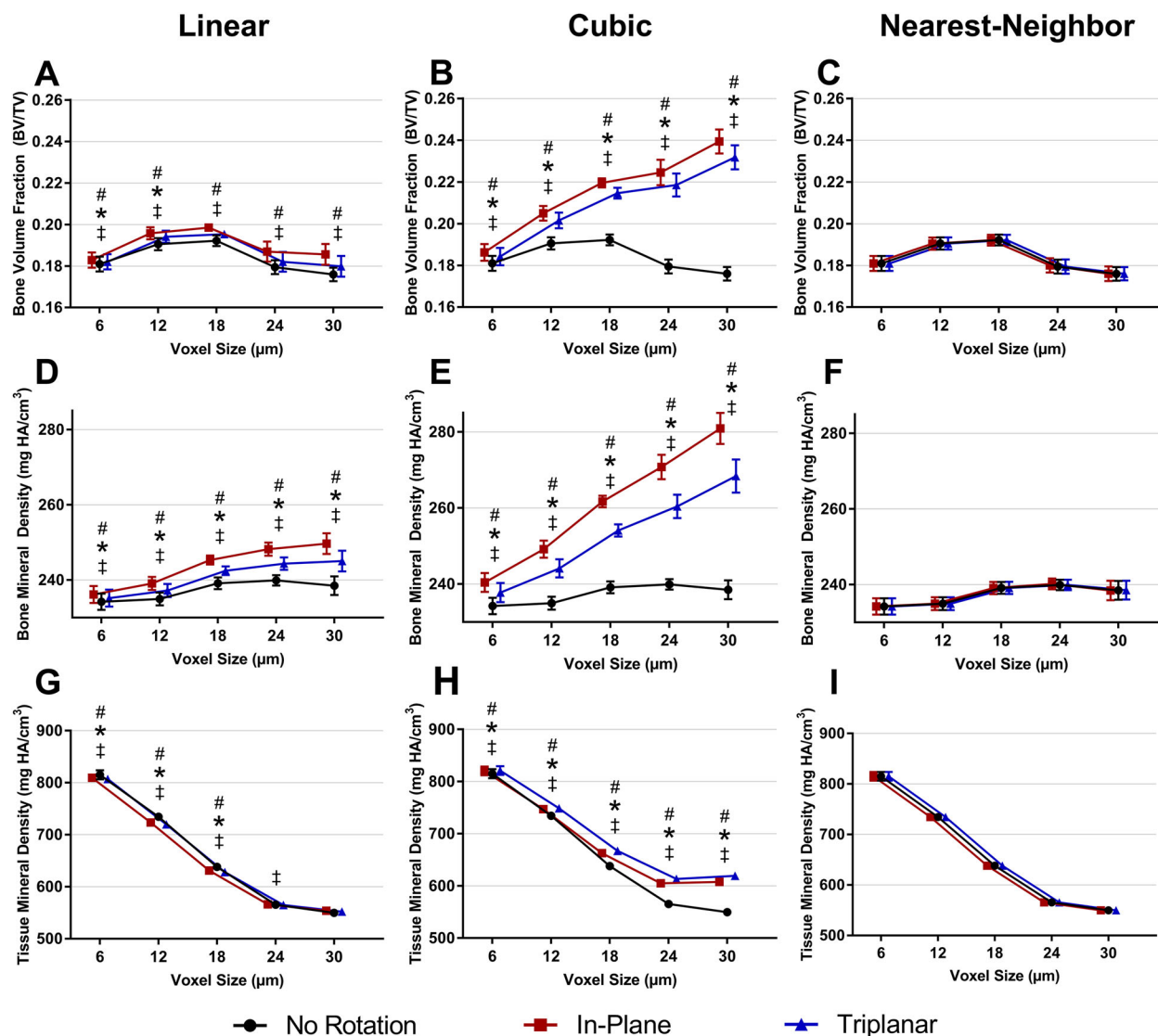


Figure 2. Effect of reorientation and interpolation type on bone volume fraction (A–C), bone mineral density (D–F), and tissue mineral density (G–I) of mouse metaphyseal trabecular bone at different resolutions. # denotes significant difference between No Rotation and In-Plane rotation at $p < 0.001$. * denotes significant difference between No Rotation and Triplanar rotation at $p < 0.001$. † denotes significant difference between In-Plane and Triplanar rotations at $p < 0.001$. Error bars represent the 95% confidence interval, calculated using the Cousineau-Moray correction for repeated measures^{4,5}.

Effect of Reorientation Type on Morphometry

Morphometric parameters were significantly affected by both In-Plane and Triplane rotations regardless of the interpolation type used, and the direction and magnitude of the error was strongly dependent on the combination of rotation and interpolation employed (Fig. 3). As with densitometric measures, in the majority of cases the magnitude of error for a given combination of measurement, rotation type, and interpolation type increased with increasing voxel size—this was particularly true for cases with higher magnitude error. Unlike densitometric measures, NN interpolation frequently produced statistically significant error, with magnitudes similar to, and in some cases higher than, Linear and Cubic interpolation. Numerous statistically significant comparisons were observed;

for brevity, only statistically significant differences with the highest magnitude percent error (Table 2) will be discussed. Error in Tb.Th was greatest using Cubic interpolation (Fig. 3A–C), resulting in significantly increased Tb.Th with mean percent differences ranging from 0.9% to 9.5%. Conversely, NN interpolation significantly decreased Tb.Th, with percent errors ranging from –1.0% to –6.2%. Error in Tb.Sp was greatest using NN interpolation, particularly after Triplanar rotation (Fig. 3D–F), however all interpolation types produced substantial error. Tb.Sp following Triplanar rotation decreased after NN (range: –4.4% to –11.8% error) and Cubic interpolation (range: –2.7% to –9.2% error). Conversely, Tb.Sp error using Linear interpolation was highest following In-Plane rotation, with increasing Tb.Sp values following Linear interpolation

Table 2. Percent Error of Mouse Metaphyseal Data Based on Voxel Size, Rotation Type, and Interpolation Type

Interp.	Rotation	Res. (µm)	BVIV	BMD	TMD	Tb.Th	Tb.Sp	TbN	SMI	
Linear	In-Plane	6	1.1% [0.9, 1.3]	0.8% [0.7, 1.0]	-0.7% [-0.9, -0.6]	1.6% [1.5, 1.8]	0.8% [0.7, 1.0]	-0.5% [-0.8, -0.3]	0.2% [-1.1, 1.5]	
		12	2.8% [2.4, 3.2]	1.8% [1.5, 2.1]	-1.5% [-1.7, -1.3]	2.2% [2.0, 2.3]	0.7% [0.5, 0.9]	0.6% [0.2, 1.0]	5.1% [4.3, 6.0]	
		18	3.3% [2.7, 4.0]	2.6% [2.2, 3.0]	-1.1% [-1.3, -0.8]	2.8% [2.6, 3.1]	3.6% [2.0, 5.2]	0.5% [0.0, 0.9]	5.3% [3.1, 7.5]	
		24	4.1% [2.7, 5.4]	3.5% [3.0, 3.9]	0.1% [-0.2, 0.4]	3.6% [3.0, 4.2]	5.8% [4.0, 7.7]	0.5% [-0.8, 1.8]	6.0% [4.3, 7.7]	
	Tri-Plane	6	0.6% [0.4, 0.8]	0.4% [0.3, 0.6]	-1.0% [-1.1, -0.8]	1.4% [1.2, 1.5]	4.5% [3.5, 5.4]	9.3% [5.9, 12.6]	4.8% [1.9, 7.7]	
		12	1.9% [1.5, 2.3]	1.0% [0.7, 1.3]	-2.0% [-2.3, -1.8]	2.1% [1.7, 2.4]	1.8% [-2.0, -1.6]	-0.7% [-1.0, -0.5]	4.5% [2.7, 6.2]	
		18	1.6% [0.9, 2.4]	1.4% [1.0, 1.8]	-1.6% [-1.9, -1.3]	2.9% [2.5, 3.2]	-0.8% [-2.7, 1.1]	-1.2% [-1.9, -0.5]	9.1% [8.2, 9.9]	
		24	1.3% [-0.2, 2.8]	1.9% [1.4, 2.3]	-0.1% [-0.4, 0.2]	3.4% [2.6, 4.2]	1.7% [-2.1, 5.5]	-2.0% [-3.6, -0.3]	10.7% [9.1, 12.4]	
	Cubic	In-Plane	6	2.2% [-0.1, 4.5]	2.8% [2.1, 3.5]	0.4% [-0.2, 1.0]	4.3% [3.0, 5.6]	3.7% [-0.3, 7.8]	-2.0% [-5.1, 1.2]	8.9% [6.5, 11.2]
			12	2.9% [2.4, 3.5]	2.7% [2.3, 3.1]	0.7% [0.6, 0.8]	1.4% [1.2, 1.6]	0.4% [0.3, 0.5]	1.5% [1.0, 2.0]	3.1% [2.1, 4.1]
			18	7.7% [6.2, 9.1]	6.1% [5.1, 7.1]	1.7% [1.5, 1.9]	2.4% [2.2, 2.7]	0.6% [0.4, 0.8]	5.1% [3.8, 6.5]	6.0% [4.0, 7.9]
			24	14.4% [12.1, 16.7]	9.5% [8.2, 10.7]	3.9% [3.3, 4.4]	3.3% [2.5, 4.0]	0.4% [-0.8, 1.6]	10.8% [8.6, 13.0]	2.2% [-0.2, 4.6]
Tri-Plane		6	25.4% [22.2, 28.5]	12.9% [11.5, 14.2]	7.1% [6.2, 7.9]	4.8% [3.7, 5.8]	-1.0% [-3.1, 1.0]	19.7% [16.4, 23.0]	-5.3% [-9.0, -1.6]	
		12	36.5% [32.0, 41.0]	17.8% [16.0, 19.7]	10.5% [9.3, 11.7]	7.5% [5.9, 9.0]	-1.1% [-4.3, 2.0]	27.1% [22.0, 32.1]	-12.1% [-16.9, -7.3]	
		18	1.8% [1.2, 2.4]	1.5% [1.1, 1.9]	0.7% [0.6, 0.8]	0.9% [0.7, 1.1]	-2.7% [-3.0, -2.4]	0.9% [0.3, 1.5]	8.6% [6.8, 10.4]	
		24	5.9% [4.3, 7.5]	4.0% [2.9, 5.0]	1.9% [1.7, 2.2]	2.2% [1.6, 2.7]	-2.9% [-3.4, -2.4]	3.7% [1.9, 5.4]	10.6% [8.6, 12.6]	
NN		In-Plane	6	11.9% [9.3, 14.4]	6.3% [4.9, 7.6]	4.6% [3.9, 5.2]	3.6% [2.7, 4.5]	-4.0% [-6.2, -1.8]	8.0% [5.7, 10.3]	5.1% [2.2, 8.0]
			12	22.1% [18.8, 25.4]	8.6% [7.2, 9.9]	8.5% [7.5, 9.6]	5.6% [4.0, 7.1]	-8.5% [-12.1, -4.9]	15.7% [12.3, 19.1]	-2.8% [-6.7, 1.1]
			18	32.2% [27.4, 37.0]	12.6% [10.5, 14.7]	12.7% [11.1, 14.2]	9.5% [7.3, 11.6]	-9.2% [-11.7, -6.7]	20.8% [15.8, 25.8]	-11.0% [-17.0, -5.1]
			24	0.003% [-0.013, 0.019]	0.008% [-0.002, 0.019]	0.002% [-0.005, 0.009]	-2.488% [-2.604, -2.372]	-1.2% [-1.2, -1.1]	2.6% [2.4, 2.7]	3.7% [2.4, 5.1]
	Tri-Plane	6	-0.008% [-0.065, 0.048]	-0.004% [-0.028, 0.019]	-0.009% [-0.042, 0.025]	-2.885% [-2.936, -2.735]	-1.9% [-2.1, -1.8]	2.9% [2.8, 3.0]	2.4% [1.4, 3.3]	
		12	-0.045% [-0.228, 0.137]	-0.023% [-0.097, 0.050]	-0.009% [-0.077, 0.059]	-2.609% [-2.829, -2.388]	-1.2% [-1.9, -0.6]	2.6% [2.3, 3.0]	4.7% [3.3, 6.1]	
		18	0.334% [-0.004, 0.673]	0.118% [0.010, 0.227]	-0.005% [-0.087, 0.076]	-1.427% [-2.065, -0.788]	0.5% [-1.9, 2.8]	1.8% [1.3, 2.2]	5.3% [3.9, 6.6]	
		24	0.009% [-0.348, 0.365]	-0.013% [-0.125, 0.098]	0.003% [-0.124, 0.129]	-1.012% [-1.612, -0.412]	0.2% [-2.1, 2.5]	1.0% [0.4, 1.7]	7.0% [4.8, 9.1]	
	Tri-Plane	6	-0.004% [-0.011, 0.003]	-0.002% [-0.006, 0.001]	0.001% [-0.003, 0.006]	-4.064% [-4.194, -3.933]	-4.4% [-4.6, -4.2]	4.2% [4.1, 4.4]	24.6% [22.7, 26.5]	
		12	0.004% [-0.022, 0.031]	0.009% [-0.002, 0.020]	0.008% [0.003, 0.013]	-6.023% [-6.277, -5.770]	-6.1% [-6.4, -5.7]	6.4% [6.1, 6.7]	8.5% [7.9, 9.1]	
		18	0.009% [-0.047, 0.065]	0.000% [-0.018, 0.018]	-0.005% [-0.026, 0.016]	-6.173% [-6.446, -5.900]	-7.5% [-8.6, -6.4]	6.6% [6.3, 6.9]	9.7% [8.9, 10.5]	
		24	-0.001% [-0.126, 0.125]	-0.006% [-0.042, 0.030]	0.001% [-0.026, 0.027]	-5.969% [-6.552, -5.385]	-10.6% [-14.3, -6.8]	6.4% [5.7, 7.0]	11.2% [10.2, 12.2]	
30	0.086% [-0.031, 0.204]	0.021% [-0.002, 0.044]	-0.009% [-0.053, 0.035]	-4.701% [-5.468, -3.933]	-11.8% [-14.4, -9.1]	5.0% [4.2, 5.9]	12.4% [10.6, 14.1]			

Data shown as mean with 95% confidence interval. Percent differences for reoriented scans were calculated with reference to the corresponding non-rotated scan at the same voxel size.

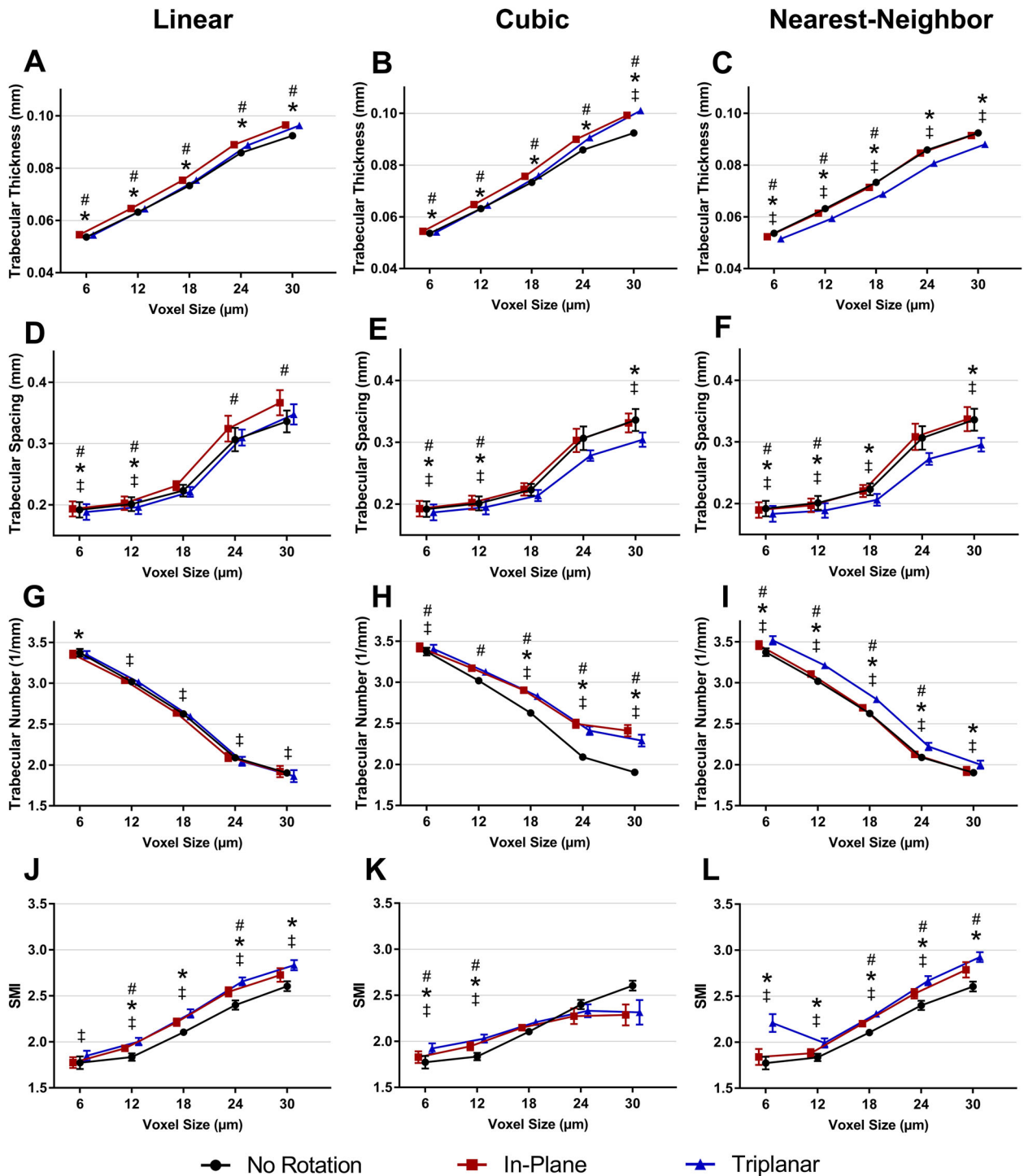


Figure 3. Effect of reorientation and interpolation type on trabecular thickness (A–C), trabecular spacing (D–F), and trabecular number (G–I), and structure model index (SMI) (J–L) of mouse metaphyseal trabecular bone at different resolutions. #denotes significant difference between No Rotation and In-Plane rotation at $p < 0.001$. *denotes significant difference between No Rotation and Triplanar rotation at $p < 0.001$. †denotes significant difference between In-Plane and Triplanar rotations at $p < 0.001$. Error bars represent the 95% confidence interval, calculated using the Cousineau–Moray correction for repeated measures^{4,5}.

(range: 0.8% to 9.3% error). Error in Tb.N was notably highest using Cubic interpolation. Tb.N increased appreciably following both Cubic (range: 0.9% to 27.1% error) and NN (range: 1.0% to 6.6%). SMI error increased following Linear (range: 0.2%

to 10.7%) and NN interpolation (range: 3.7% to 24.6%) and exhibited resolution dependent changes following Cubic interpolation (range: 3.1% to –12.1%), with increasing and decreasing SMI observed at higher and lower resolutions, respectively.

DISCUSSION

Reorientation of μ CT datasets is commonly employed during analysis of bony tissues to facilitate ROI selection, image registration, and computation of 2D metrics such as moment of inertia, but, to date, the effects of these algorithms on densitometric and morphometric measurements have not been characterized. This study aimed to characterize the error produced by commonly employed reorientation algorithms as a function of interpolation type, plane of rotation, and voxel size. Our data demonstrates that both densitometric and morphometric parameters of bone tissues are significantly affected by reorientation. Furthermore, the magnitude of error for a given parameter is highly dependent on the interpolation type, rotation plane, and interactions of these two variables with voxel size.

Although attempts are generally made to standardize sample positioning during μ CT experiments, completely consistent orientation is often difficult and infeasible, and reorientation of μ CT datasets prior to analysis is extremely common in bone research. Our data show that rotation of any kind causes statistically significant changes to both densitometric and morphometric parameters. The magnitude of error due to reorientation was highly dependent on voxel size. Generally, our data indicates that high resolution imaging (6 or 12 μ m for mice) produced relatively low magnitude error, though certain parameters such as BV/TV, Tb.N, and SMI exhibited errors of 4–9% even at these high resolutions. Scans taken at lower resolutions (24 or 30 μ m) could produce substantial error—for example, BV/TV and Tb.N of 30 μ m scans increased by an average of 36.5% and 27.1%, respectively, following In-Plane rotation with Cubic interpolation. Christiansen⁶ has previously demonstrated that increasing voxel size has a substantial independent effect on both densitometric and morphometric parameters, and our results corroborate this finding. Our data further shows that there is an additional, interactive effect whereby high voxel sizes exacerbate the error caused by image reorientation. It is important to note that the percent errors measured in this study were calculated *within* each voxel size, and thus these errors reflect the isolated effect of the reorientation algorithm and not the independent effects of voxel size characterized by Christiansen. Specifically with regards to thickness calculation, Saha et al.⁷ recently demonstrated a “fuzzy distance transform” (FDT) method for trabecular thickness determination designed to address the issue of volume averaging in bone images acquired at relatively low resolutions. Compared to the commonly employed binary segmentation and direct distance transform-based thickness computations assessed in this study, FDT represents a possible alternative in situations where significant volume averaging of trabeculae is expected. In the two samples assessed in their study, in-plane

rotations with linear interpolation introduced maximum errors of 3.3% and 4.5%, respectively, suggesting that rotation error is still a consideration if FDT is used for thickness determination.

Interpolation type played a large role in determining the reorientation error. Our data indicate that NN interpolation created considerable morphometric error, but almost no densitometric error. NN interpolation does not create new intensity values, but simply re-assigns values from the original to the reoriented image. This results in considerable geometric distortion, reflected by the high morphometric error. However, it results in very little change in the intensity distribution of the image, and subsequently in the distribution of intensities which meet the bone threshold, resulting in well conserved densitometric computations as densitometry is directly computed from bone voxel intensities and is independent of geometry/spatial arrangement. Linear interpolation generally caused measurable but low magnitude error in all measurements, particularly at low voxel sizes, and may be the best overall choice when both densitometry and morphometry are being computed. Cubic interpolation was found to cause relatively high error in most cases, particularly in densitometric parameters (BV/TV and BMD), and this error was particularly exacerbated at higher voxel sizes. Unlike NN and Linear interpolations, Cubic interpolation can produce intensities outside the range of neighboring voxels—this may explain why Cubic interpolation caused the greatest alterations in densitometric measurements. In practice, it is common for VOI selection to be performed on reoriented images. In order to produce maximally consistent data, we used a single VOI for each original image and mapped this VOI to the reoriented images, and thus our data does not consider the effect of interpolation type on the accuracy of manual or automated VOI selection. Generally, Cubic interpolation is known to produce the smoothest resultant image and is the standard interpolation type in many commercial image editing programs (i.e., Adobe Photoshop), with “stair-step” artifacts becoming increasingly pronounced using Linear and NN interpolation, in order. These more “qualitative” aspects of reorientation error should be carefully weighed against quantitative measurement error when selecting a reorientation algorithm in the context of a given study.

Both In-Plane and Triplanar rotations caused statistically significant error in most conditions. Interestingly, however, In-Plane rotation generally caused higher error in densitometric parameters, while Triplanar rotation caused higher error in morphometric parameters. This difference is likely due to nature of the interpolation algorithms employed, along with inherent differences in densitometric and morphometric measures. As described above (Table 1), each interpolation algorithm is based on 3-dimensional proximity. During In-Plane

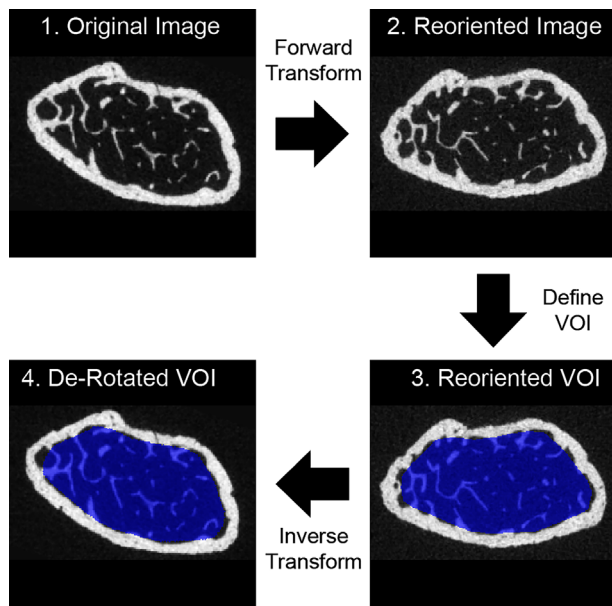


Figure 4. Schematic illustration of image de-rotation. A misaligned image (1) is captured and subsequently reoriented (2). VOI contouring is performed on the reoriented image (3), and the VOI is then de-rotated to align with the original image (4). A MATLAB implementation of this strategy is available on the MATLAB File Exchange.

rotation, the reoriented and original images remain precisely aligned in the axial plane, thus NN interpolation will always select an in-plane voxel, and out-of-plane voxels will be assigned no weight in Linear and Cubic interpolations; in effect, perfectly In-Plane rotation results in in-plane, 2D interpolation, whereas Triplanar rotation results in interpolation using the full 3D neighborhood of voxels. To our knowledge, this is not a specific quality of the MATLAB implementation of these algorithms, but rather quality inherent in the interpolation algorithms employed. We hypothesize that attenuation data (and thereby densitometry) is more accurately interpolated with Triplanar rotation compared to In-Plane rotation, particularly at border regions, because the full 3D voxel neighborhood is incorporated into the average rather than only the 2D in-slice neighbors. Conversely, morphometry is less sensitive to intensity values but highly dependent on geometry/spatial arrangement. Because morphometry is being calculated on discretized data (implying an inherent “stair step” at border regions), orientation is important to consistency, particularly with high voxel sizes where the stair step is larger with respect to anatomic feature size. It is intuitive that reorientation in all three planes (e.g., Triplanar rotation) causes more geometric distortion and, thereby, higher morphometric error. To ensure all reorientations were computed consistently, both In-Plane and Triplanar rotations were done utilizing 3D rotation matrices and the MATLAB “imwarp” function. Though our results are computed using the MATLAB implementation of these three interpolation

algorithms, we expect results to be similar in other softwares due to the well-defined and conserved nature of the interpolation algorithms employed. Certain morphometric parameters calculated in this study (i.e., Tb.N) have multiple definitions based on the model being assumed, and we cannot comment on how these alternative computations would change our findings.

In this investigation, we simulated image reorientation by capturing properly aligned original images and then performing prescribed rotations on them. This was done to enable VOI placement (1) on original scans and (2) on a consistent reference frame to limit variability in VOI placement. It is worth noting that in most practical applications, the reverse is the case: A misaligned image is captured and subsequently rotated to reorient to a desired view. However, we would assert that the act of interpolating, and not the specific beginning/ending orientation of the scan, drive reorientation error. This is supported by our preliminary analysis, which indicated that the angle of rotation did not meaningfully impact the magnitude or direction of reorientation error. Thus, it seems reasonable to conclude that our results would have been similar if the scans had been acquired off-axis and then reoriented. As all of our VOIs were acquired on properly aligned scans, we cannot comment on the extent to which VOI placement on misaligned images affects analysis of trabecular bone, nor on the relative magnitude of reorientation-caused and VOI placement-caused error. We analyzed only trabecular bone in this study and therefore can only surmise as to how these results translate to analysis of cortical bone. However, our analysis of trabecular bone showed that error due to rotation was highly dependent on resolution. Specifically, reorientation error was exacerbated when resolution was insufficient relative to feature size. Since cortical bone is generally thicker than trabecular bone, it presumably follows that any image acquisition and analysis strategy considered sufficient for analysis of trabecular bone in a given model should be sufficient for cortical analysis.

Regardless of the interpolation type and plane of rotation, reorientation produced statistically significant error in bone densitometry and morphometry. However, with sufficiently image high resolution, the magnitude of this error is generally small and may be acceptable for a particular study if expected differences between study groups are large enough. Reorientation error in a given study may be further minimized by selecting the appropriate interpolation type. In studies assessing only densitometry NN interpolation is recommended, whereas Linear interpolation is recommended if both densitometry and morphometry are being computed. If maximal image smoothness is desired, Cubic interpolation can be employed; however care should be taken to ensure sufficient resolution to limit reorientation error, particularly in densitometric data. Investigators seeking to

totally avoid reorientation error should attempt to circumvent the need for reorientation through rigorous sample positioning during scanning. If this is not possible, an alternative approach is to capture the image, reorient the image for VOI selection and save the transformation used, manually or automatically select the VOI on the reoriented image, and then “de-rotate” the VOI back onto to the original image using the inverse transformation (Fig. 4). This approach is more labor intensive, however it provides multiple advantages: Quantitative analysis can be performed on the original image and thus avoid reorientation error, while manual or automatic VOI selection can be performed on the reoriented image and thus enable maximal consistency, and interpolation type can then be selected to ensure maximal visual image quality without consideration of reorientation error. We have provided a MATLAB implementation of this strategy, which is available on the MATLAB File Exchange. Finally, if image reorientation is utilized at all in a study, it should be utilized for all samples, regardless of whether they are positioned correctly initially, and should be done using a consistent algorithm to ensure consistent interpolation type and planes of rotation to ensure that any error introduced is consistent throughout all samples.

AUTHORS' CONTRIBUTION

All authors were involved in research design, acquisition, analysis, and interpretation of data, and have read and approved the final submitted manuscript.

ACKNOWLEDGMENTS

This research did not receive any specific grant from funding agencies in the public, commercial, or not-for-profit sectors.

REFERENCES

1. Bouxsein ML, Boyd SK, Christiansen BA, et al. 2010. Guidelines for assessment of bone microstructure in rodents using micro-computed tomography. *J Bone Miner Res* 25: 1468–1486.
2. Doube M, Kłosowski MM, Arganda-Carreras I, et al. 2010. BoneJ: free and extensible bone image analysis in ImageJ. *Bone* 47:1076–1079.
3. Sage D, Prodanov D, Tinevez J-Y, et al. MIJ: making interoperability between ImageJ and Matlab possible, ImageJ User & Developer Conference, 2012.
4. Morey RD. 2008. Confidence intervals from normalized data: a correction to Cousineau (2005). *Tutor Quant Methods Psychol* 4:61–64.
5. O'Brien F, Cousineau D. 2014. Representing error bars in within-subject designs in typical software packages. *Quant Methods Psychol* 10:56–67.
6. Christiansen BA. 2016. Effect of micro-computed tomography voxel size and segmentation method on trabecular bone microstructure measures in mice. *Bone Rep* 5:136–140.
7. Saha PK, Wehrli FW. 2004. Measurement of trabecular bone thickness in the limited resolution regime of in vivo MRI by fuzzy distance transform. *IEEE Trans Med Imaging* 23: 53–62.

SUPPORTING INFORMATION

Additional supporting information may be found online in the Supporting Information section at the end of the article.